

Full paper

Rationally designed rotation triboelectric nanogenerators with much extended lifetime and durability



Zhiming Lin ^{a,b,1}, Binbin Zhang ^{b,1}, Haiyang Zou ^{b,1}, Zhiyi Wu ^{a,b}, Hengyu Guo ^b, Ying Zhang ^b, Jin Yang ^c, Zhong Lin Wang ^{a,b,*}

^a Beijing Institute of Nanoenergy and Nanosystems, Chinese Academy of Sciences, Beijing, 100083, PR China

^b School of Materials Science and Engineering, Georgia Institute of Technology, Atlanta, GA, 30332-0245, United States

^c Key Laboratory of Optoelectronic Technology & Systems (Ministry of Education), Department of Optoelectronic Engineering, Chongqing University, Chongqing, 400044, PR China

ARTICLE INFO

Keywords:

Triboelectric nanogenerator
Transmission mechanism
Long-time operation
Durability

ABSTRACT

Triboelectric nanogenerators (TENG) is a promising route for harvesting ambient mechanical energy to obtain clean and renewable electricity. However, the durability of materials still limits its practical applications for continuous operation. Here, a radial-arrayed TENG was integrated with a transmission mechanism, which successfully maximized the sustainable operation with less triboelectric material wear and damage. Through the rational design of the transmission mechanism, triboelectric layers were first charged by the contact electrification due to the wave impact from the sides, and charges were transferred by the electrostatic induction continuously because of the tumbler's design. In this case, frictional resistance between the triboelectric layers were successfully eliminated, which largely enhances its robustness and durability. After running for 500 k cycles, there is only 1.8% degradation. The TENG could convert one single impact into multiple cycles of rotations, which improves the energy harvesting efficiency for sustainably driving and charging commercial electronics, immediately demonstrating the feasibility of the TENG as a practical power source with extended lifetime and durability. Given exceptional durability and unprecedented applicability resulting from novel designs, this work provides an attractive strategy for the study of triboelectric nanogenerator's durability and facilitates the development of the self-powered systems.

1. Introduction

A rapid progress of microelectronics, information technology and Internet of Things (IoT) is predicted to change the human's life all around the world [1–6]. A key challenge in achieving these goals is the need to develop integrated sustainable power sources into the IoT systems to support the ubiquitous and mobile operation of sensing nodes, since the traditional batteries inevitably require periodic replacement or recharging and have potential environmental pollution [7,8]. So harvesting ambient energy as a continuous and self-sufficient energy source is considered as a reliable and independent strategy for such electronic devices [9–11]. Various technological approaches have been put forward to efficiently convert ambient energies into electric power, such as piezoelectric [12,13], thermoelectric [14,15], and triboelectric effects [16,17]. Triboelectric nanogenerator is characterized by the high output

voltage, light-weight, high power density, environmental friendliness, and diverse choice of materials as a continuous and self-sufficient energy source [18–26]. Extensive efforts have been made to fabricate various TENGs for obtaining different energy in environments [27–33]. Nevertheless, the frictional force between the two triboelectric materials would lead to output degradation because of the material's wear and surface damage. No fundamental approach has yet been proposed for the solving the durability and stability of the TENG. Although Guo et al. [34] presented a high-performance TENG on the basis of charge replenishment by introducing a rod rolling friction in the structure design. However, the frictional force between the rod and triboelectric layer will lead to the degradation of the surface morphologies. Therefore, attaining extreme robust and durable TENG without material abrasion for long-time operation is still a challenge.

Herein, we presented a strategy to maximize the TENG's durability

* Corresponding author. Beijing Institute of Nanoenergy and Nanosystems, Chinese Academy of Sciences, Beijing, 100083, PR China.

E-mail address: zhong.wang@mse.gatech.edu (Z.L. Wang).

¹ These authors contributed equally to this work.

by a conjunction of a transmission mechanism and radial-arrayed TENG. In the protocol, an external trigger on a flabellum drives two triboelectric materials of the TENG's rotor and stator to physically contact, which will produce triboelectric charges respectively on the two surfaces. Under external disturbances, the charged TENG's rotor could periodically swing without any contact as a simple pendulum, which well significantly reduced the material abrasion and largely enhanced the device's durability. Owing to the innovative design of pendulum rotor, the TENG presents frequency-multiplied output performance at a low driving frequency, largely improving energy-conversion efficiency. Furthermore, the practical applicability of the TENG for long-time operation as a power source is demonstrated, and the energy scavenging from water wave can be stored in a capacitor and to drive a digital sensor. Given the superior device robustness and high-performance electric output, adapting this methodology will aid in the development of stable energy-harvesting research as well as further promote the applications of TENGs for engineering applications.

2. Results and discussion

2.1. Structure design

As sketched in Fig. 1a, a TENG has been fabricated to scavenge water wave energy to demonstrate the feasibility of this method. The device has two major motion parts: a transmission motion part and radial-arrayed rotation part, as schematically illustrated in Fig. 1b. The transmission mechanism consists of a flabellum, an acrylic rod, and a spring. The acrylic rod connects the flabellum and spring. The flabellum could convert the wave force from various directions into one single direction of movement to press the rod and compress the spring. And the rotor fixed at the acrylic rod with a center bearing is a radially-arrayed sector of nylon materials separated by equal-degree intervals. An iron mass was installed in the back edge of the rotor to form a tumbler-like structure, so that the rotator section swing like a pendulum, as shown in the inset in Fig. 1b. The stator with the same dimensions of the rotor is fixed with the

outer cylinder shell. It has a three-layer structure: a polytetrafluoroethylene (PTFE) film as a triboelectric material, an electrodes plate with a complementary electrode and an acrylic substrate. There exists a tiny gap (~ 0.5 mm) between the rotator and stator, namely, the free-standing gap for the rotor's rotation to swing without any frictional force. Thus, this structure design not only is sensitive to external mechanical excitation but also accounts for excellent durability, making the TENG practically reliable and robust. The photographs of the as-fabricated TENG, rotor, and stator are exhibited in Fig. 1c. Additionally, to further enhance the output performance of the TENG, nanostructures on the PTFE surface were created through the inductively coupled plasma (ICP) etching treatment, as shown in Fig. 1d. The detailed fabrication process was presented in the Experimental Section.

2.2. Electricity generation process

The operation mechanism of the as-fabricated TENG based on the unique conjugation of contact electrification and electrostatic induction is schematically illustrated in Fig. 2, which demonstrates the charge transfer process of the device under short-circuit condition. At original state, supposing there are no original charges on the surfaces of the triboelectric layers, as depicted in Fig. 2a(i). When an external trigger such as the water wave is applied to the TENG, the flabellum will turn the force from various directions into one single direction of movement to press the rod and compress the spring. And the rotor fixed at the transmission rod will naturally contact with the stator, as shown in Fig. 2a(ii). An equal amount of negative and positive charges will be, respectively, generated on the surfaces of PTFE film and the nylon film due to the difference of the electron affinity between two triboelectric materials [35]. Then the spring returns to its original position, resulting in the separation of the charged rotor and stator, as depicted in Fig. 2a(iii). This is the automatic process of the contact electrification for the device.

Due to the disturbance or tiny waves generated by water wave, the charged TENG's rotor could periodically swing without any frictional force as a simple pendulum along the axis. We define the initial state as the rotator is aligned with electrode A. The positive charge density on

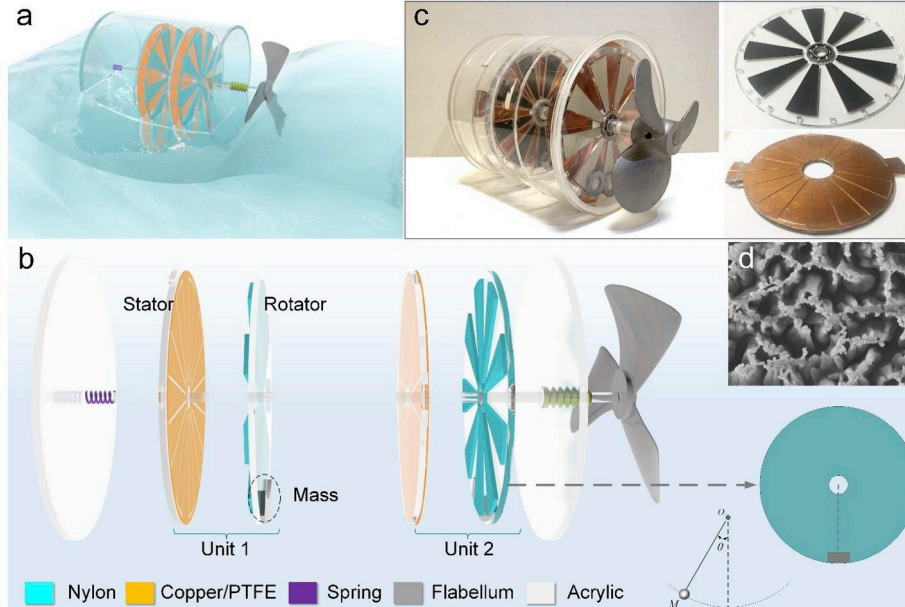


Fig. 1. Structural design of the triboelectric nanogenerator for ocean energy. (a) Schematic illustration of the triboelectric nanogenerator in water. (b) Schematic diagram of the triboelectric nanogenerator composed of stators, rotators, spring, and flabellum. (c) Photograph of the fabricated TENG, a rotator, and a stator. (d) SEM images of the etched PTFE film.

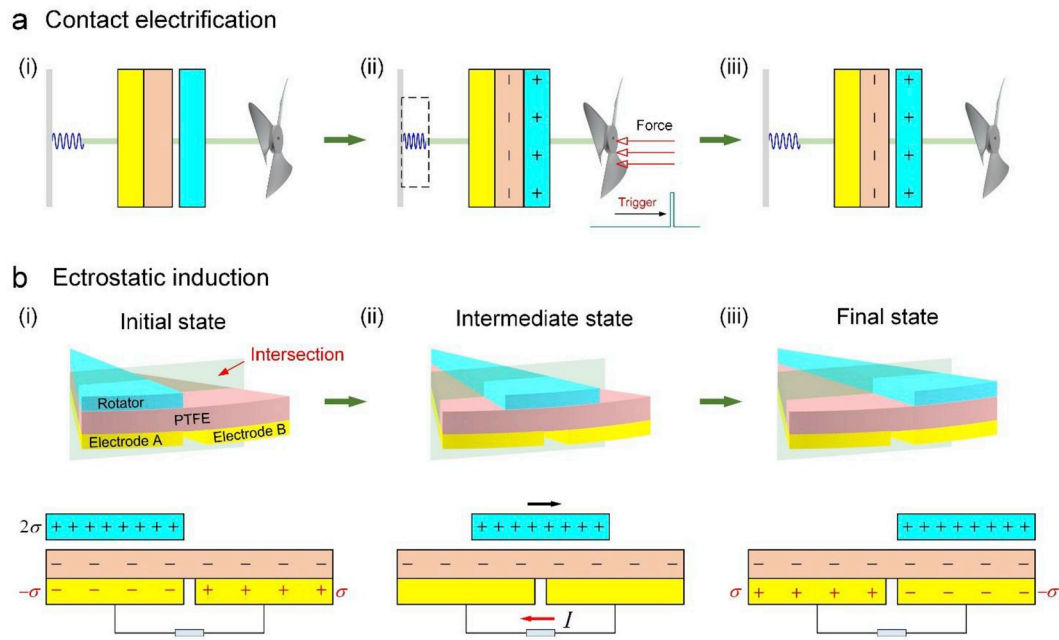


Fig. 2. Schematics of the operating principle of the triboelectric nanogenerator. (a) The contact electrification for (i) TENG at non-charged state, (ii) TENG charged by external trigger force, and (iii) TENG at charged state. (b) The electrostatic induction for (i) the initial state in which the rotator is in alignment with electrode A (The three sections from top to bottom illustrate the three-dimensional schematic, charge distribution in short-circuit condition), (ii) the intermediate state in which the rotator is spinning away from the initial position, and (iii) the final state in which the rotator is in alignment with electrode B.

the rotator is twice as much as that of negative ones on the stator owing to contact area difference, as illustrated in Fig. 2b(i). Ideally, due to the electrostatic induction, there will induce an equal amount of negative and positive charges distributed on the electrode A and B, respectively. Once the nylon film on the rotor slides from electrode A toward electrode B, the electrons will flow from electrode A to electrode B though the external load to balance a potential difference, as demonstrated in Fig. 2b(ii). When the nylon film reaches the overlapping position of electrode B at the final state, an equal amount of negative and positive charges is distributed on the two electrodes (Fig. 2b(iii)). And further

sliding beyond the final state will generate a reversed current due to the periodical structure. Furthermore, the free-standing gap between rotor and stator is beneficial to the periodically rotation, leading to a multiple output performance at a low-frequency exaction. Owing to the automatically charged process and the free-standing gap, the triboelectric material abrasion is successfully minimized, resulting in the supreme robustness and ultralong lifetime of the above TENG.

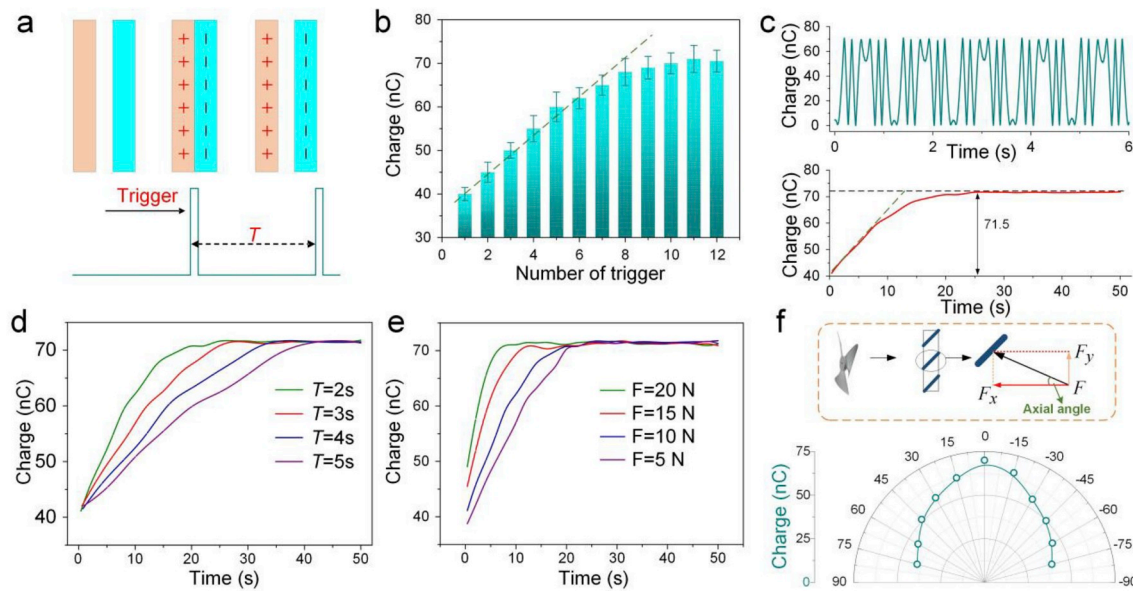


Fig. 3. Factors that influence the transferred charge quantity of the TENG. (a) Schematic of external trigger from water wave. (b) The transferred charge quantity at different triggers. (c) The detailed output charge curve, and the transferred charge quantity at versus trigger cycles. (d) The dependence of the transferred charge performance on various time of intervals. (e) The dependence of the transferred charge performance on various forces. (f) The transferred charge performance for different trigger angles at the force of 5 N.

2.3. Electrical characterization

As is well-known, the amount of transferred charges is one of the most important parameters of triboelectric nanogenerators since it directly determines the output performance. Here, a programmable linear motor is applied as an external exaction to provide a periodic trigger, as shown in Fig. 3a. Firstly, we investigated the change of the transferred charge amount with a periodic trigger at the force of 10 N, as demonstrated in Fig. 3b. The transferred charge amount increases rapidly in the first ten triggers and then reaches a steady value in the following triggers. Fig. 3c (top panel) shows the detailed output charge curve at the saturated state, which depicted multiple output charges for single trigger due to the radial-arrayed structure design. And Supplementary Fig. S1 demonstrates the corresponding output voltage and current with the multiple output characteristics. Additionally, Fig. 3c (bottom panel) shows the accumulated charge amount for the TENG by the continuous triggers with the interval time of 2 s, it can be seen that the efficient charge amount linearly increases in the initial stage, and then increases slowly after ten triggers, and reaching a saturated state with the charge amount of 75 nC. We also explored the interval time (T) of the trigger on the accumulated charge amount, as demonstrated in Fig. 3d. A smaller interval time (T) contributes to reaching the saturated state faster, since the trigger number is increased in unit time. The trigger force on the accumulated charge amount was systematically investigated, as shown in Fig. 3e and f. The charge amount increases with the elevation of the axial force, and a larger force leads to a faster growth rate (Fig. 3e). As the increase of the force would lead to a better contact between the triboelectric materials, and result in a larger tribo-charges. Fig. 3f illustrates the accumulated charge amount at different trigger angles of the axial force with the same values. With the axial angle increase, the accumulated charge amount decreased dramatically due to the axial force F_x reduced, and the output voltage also shows the same trend, as depicted in Supplementary Fig. S2.

To comprehensively investigate the electrical output performance of the TENG, the influence of the acceleration of external excitations on the performance of the TENG was studied, as demonstrated in Fig. 4a. The amplitude of output voltage remains stable, which is independent of the acceleration since it is only determined by the charge density. In comparison, the output current increases with the enhancement of the

exaction acceleration, because a larger exaction acceleration shortens the cycle time, so that a certain amount of electrons flow in a shorter time. Moreover, a single excitation on the TENG would lead to a long time of rotation, as long as 22 s, until the rotor eventually comes to rest, rendering a long-term and frequency-multiplied output performance due to the pendulum-like structure without any frictional force for operation, which largely enhances the energy harvesting efficiency, as demonstrated in Fig. 4b. This result shows that this TENG has outstanding energy harvesting capability for the low-frequency excitation. Various load resistances were connected to the TENG, and the output current and power across the resistor were measured, as demonstrated in Fig. 4c. The measured maximum output power reaches to 74 μ W with the matched resistance of 100 M Ω . And the instantaneous output power at its matched resistance and the produced energy for a single excitation were also demonstrated in Fig. S3. Besides, Supplementary Fig. S4 also illustrates the charging performances of the TENG for different capacitors, showing an excellent energy collection ability.

Importantly, the TENG based on the special designed rends exceptional durability in regards to external mechanical stimuli. We firstly investigated the behavior of the accumulated charge amount for a long-term working condition, as illustrated in Fig. 4d and Supplementary Fig. S5. The accumulated charge amount just decays 12.8% for the operation time of 10 min without any charge process, showing a super ability of long-term charge retention, which largely contributes to the stable output of TENG, especially for the ultra-low frequency excitations. A further step was taken to test the output durability of the TENG at an interval time (T) of 2 s for one trigger, as shown in Fig. 4e and Supplementary Fig. S6. It is found that in spite of tiny deviation at the original state, the voltage signal stayed stable within a total of 500 k working cycles (Attenuation: 1.8%), indicating the excellent sturdiness and durability of the device. The super durability of the TENG is beneficial from the creative structural mechanism, the frictional resistance between the triboelectric layers and the material's abrasion are significantly minimized. In this regard, it is convincing that the performance of as-fabricated TENG is capable and reliable for long-term service.

2.4. Applications

Given the features of the simple structure, low-cost, excellent

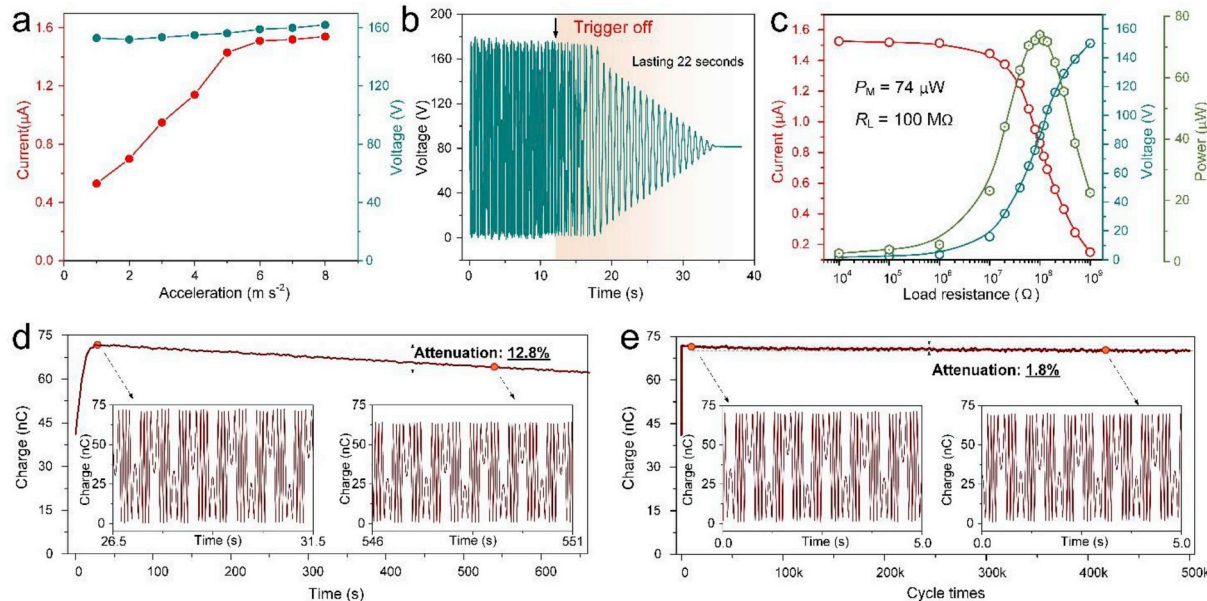


Fig. 4. The output performance of the TENG. (a) Open-circuit voltage and short-circuit current at different accelerations. (b) The lasting time of the output voltage for a trigger. (c) The current, voltage and power output of SCE-TENG with voltage stabilization under various external load. (d) The performance of the charge amount for long-term operations without charge process. (e) The durability of the TENG over various cycles.

durability and compatibility, the TENGs are possible large-scale manufacturing and applied to the large-scale energy generation. Fig. 5a illustrates the TENG arrays for large-scale energy harvesting, in which each TENG is individually rectified then parallelly connected to power the sensor nodes. Furthermore, multi-radial-arrayed TENGs could be embedded into one device to elevate the electrical output, resulting in the enhancement of the power density, as illustrated in Fig. 5b. The output current of the device with two radial-arrayed TENGs is twice as large as the current of the device with one, but the output voltages of the devices are almost the same values due to the parallel design (Supplementary Fig. S7). Besides, the charging performances for different radial-arrayed TENGs in a device was also demonstrated that the charging rate increases with the number increase of the radial-arrayed TENGs, as depicted in Fig. 5c. The device with two units can charge the capacitor to 6.8 V in 60 s, but the device with a single unit could only charge to 3.6 V within the same time.

Water wave energy is the largest estimated global resource form of renewable energy, however, it is a great challenge to harvest the ocean energy efficiently at low cost due to the low-frequency motion and the form of local oscillating motions in small regions at most of the time. The proposed TENG is deemed to be a promising way to exploit the wave energy efficiently. Fig. 5d shows an imagine screen of the TENG arrays for large-scale water wave energy harvesting. Hundreds of unit were parallelly connected to scavenge water wave energy. Various applications of the TENG in water wave energy harvesting have been demonstrated. Fig. 5e demonstrated the utilization of the electrical energy obtained by the developed TENG from the water wave to power the light-emitting diodes (LEDs). The word “OCEAN” composed of 55 LEDs can be lighted up by the TENG continuously by a single device (see Supplementary Video S1). Moreover, the TENG also can drive the sensor nodes in the environment to form a self-powered monitoring system. Fig. 5f and Supplementary Video S2 illustrated the photograph and video of the digital thermometer successfully powered by the developed TENG. These applications indicate the capability of the developed TENG in converting environment energy for self-powered systems as well as possibility for generating electricity at a large scale.

Supplementary video related to this article can be found at <https://doi.org/10.1016/j.nanoen.2019.104378>.

[://doi.org/10.1016/j.nanoen.2019.104378](https://doi.org/10.1016/j.nanoen.2019.104378).

3. Conclusions

In summary, we proposed a rational strategy to boost the durability of TENG by integrating a radial-arrayed TENG with a transmission mechanism, achieving the continuous operation for long-term service. The transmission mechanism makes the process of the contact electrification automatically and periodically, and radial-arrayed TENG with pendulum-like structure could work without triboelectric material abrasion due to the free-standing gap between rotor and stator, which not only could scavenge ambient energy but also features the advantages of frequency-multiplied output performance as well as excellent robustness and durability of the device. Systematical investigations of the dependence of charge amount on the interval time, force and directions of external triggers were studied comprehensively to obtain a thorough understanding of the charging process. In addition, the developed TENG array was employed to harvest water wave energy to continuously power a thermometer, which provides a possible green method to construct marine self-powered systems. Benefiting from the advantages of supreme robustness, and frequency-multiplied output, this work presented a straightforward and effective solution to address the robustness and durability of the TENG for continuous operation, which should be immediately and extensively adopted in large-scale energy harvesting as well as extensive applications in self-powered hydrological sensing systems.

4. Experimental section

Fabrication of the TENG. For the transmission mechanism, an acrylic rod with the diameter of 10 mm was tailored by laser cutting (PLS6.75, Universal Laser Systems) as the transmission bar. A spring with an inner diameter of 10 mm was mounted at one end of the acrylic rod, then a metal flabellum was fixed the other end of the acrylic rod to sense the external exactions. For the radial-arrayed TENG, two acrylic sheets were cut into two disks as the substrates with a diameter of 13 cm and 12 cm, respectively. Then the patterns of the two sets of

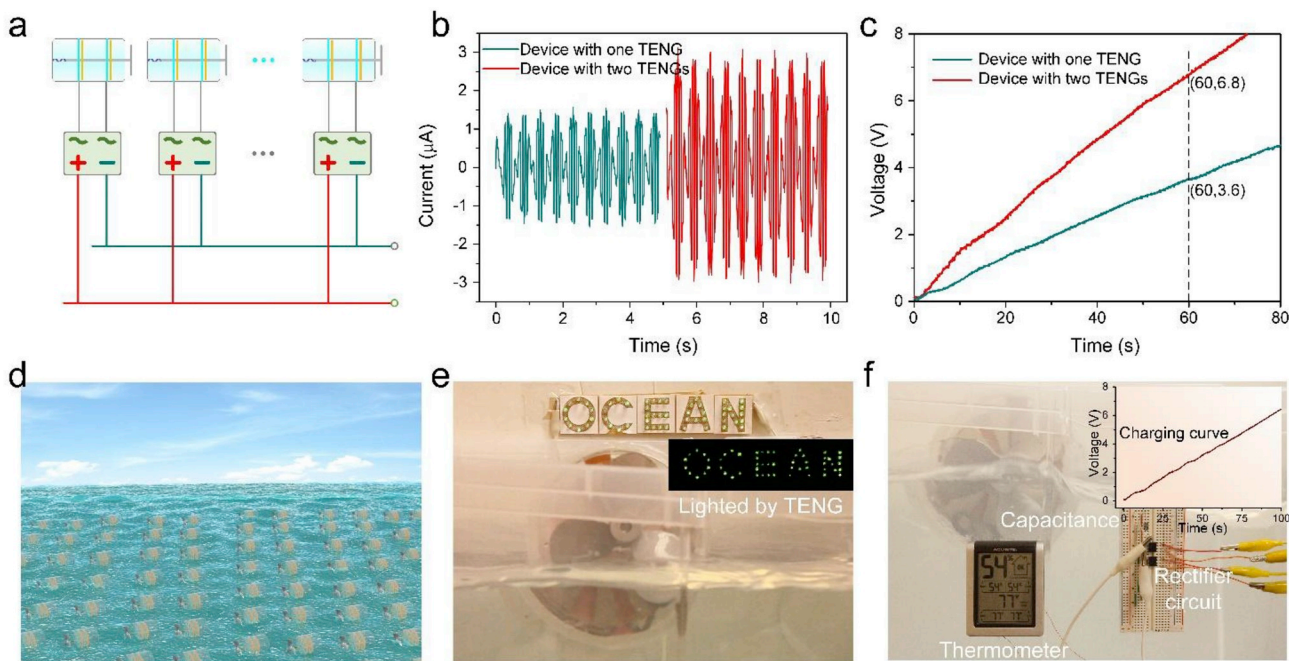


Fig. 5. Output performance of the TENG array and applications. (a) Schematic diagram of the rectification circuit for the array. (b) Comparison of the TENG with one and two disk-TENG units, and (c) the charging performance to a capacitor of $10 \mu\text{F}$. (d) Imaginary picture of future large-scale TENG networks for harvesting water wave blue energy. (e) Photograph of the TENG to power a serial LED. (f) Photograph of the TENG to power a thermometer.

complementary radial-arrayed strips on these two disks were tailored by laser cutting. A layer of Cu was deposited on the surface of the disk with diameter of 13 cm as the electrodes, and then a thin layer of FTFE was adhered onto the electrode layer as the negative triboelectric layer. The nylon strips were adhered onto the disk with a diameter of 12 cm as the positive triboelectric layer. The disk with a diameter of 12 cm was drilled a center-through hole to mount a bearing, and fix a mass at the edge of the disk. Finally, a cylinder with an inner diameter of 13 cm was prepared, and the disk (13 cm) was fixed in the cylinder vertically. Then the disk (13 cm) was mounted on the acrylic rod and put the whole part into cylinder. Two tailored acrylic disks were then adhered on both ends of the cylinder for sealing.

Characterization and measurements. The as-fabricated TENG was mounted on the programmed linear motor which was used to simulate the external exactions, and another linear motor with a force meter at the tip was used to provide the specified trigger force to the flabellum. The output voltages and transferred charges of the TENG were measured by the low-noise voltage preamplifiers (Keithley 6514 System Electrometer) and the output currents were tested by Stanford Research System SR570. A programed LabVIEW interface was used to realize real-time data acquisition.

Author contributions

Z.L.W. and Z.L. conceived the idea, Z.L., B.Z. and Z.L.W. analysed the data and wrote the paper. Z.L., B.Z., Z.W., and J.Y. fabricated the P-TENG and did electric measurement. H.G. and J.Y. optimized the structure of the TENG. H.Z. helped with the manuscript. All the authors discussed the results and commented on the manuscript.

Declaration of competing interest

The authors declare no competing financial interests.

Acknowledgements

The authors acknowledge support from National Natural Science Foundation of China (NSFC No. 51576161), and 111 project (B16038). Z.L. thanks China Scholarship Council for supplying oversea scholarship.

Appendix A. Supplementary data

Supplementary data to this article can be found online at <https://doi.org/10.1016/j.nanoen.2019.104378>.

References

- [1] W. Gao, S. Emaminejad, H.Y.Y. Nyein, S. Challa, K. Chen, A. Peck, H.M. Fahad, H. Ota, H. Shiraki, D. Kiriyama, Nature 529 (2016) 509–514.
- [2] A. Chortos, Z. Bao, Mater. Today 17 (2014) 321–331.
- [3] Q. Hua, J. Sun, H. Liu, R. Bao, R. Yu, J. Zhai, C. Pan, Z.L. Wang, Nat. Commun. 9 (2018) 244.
- [4] H. Lee, T.K. Choi, Y.B. Lee, H.R. Cho, R. Ghaffari, L. Wang, H.J. Choi, T.D. Chung, N. Lu, T. Hyeon, Nat. Nanotechnol. 11 (2016) 566–572.
- [5] T. Yokota, P. Zalar, M. Kaltenbrunner, H. Jinno, N. Matsuhisa, H. Kitano, Y. Tachibana, W. Yukita, M. Koizumi, T. Someya, Sci. Adv. 2 (2016), e1501856.
- [6] M.J. Cima, Nat. Biotechnol. 32 (2014) 642–643.
- [7] D. Larcher, J.-M. Tarascon, Nat. Chem. 7 (2015) 19–29.
- [8] S. Wang, Z.-H. Lin, S. Niu, L. Lin, Y. Xie, K.C. Pradel, Z.L. Wang, ACS Nano 7 (2013) 11263–11271.
- [9] S. Chu, A. Majumdar, Nature 488 (2012) 294–303.
- [10] J. Baxter, Z. Bian, G. Chen, D. Danielson, M.S. Dresselhaus, A.G. Fedorov, T. S. Fisher, C.W. Jones, E. Maginn, U. Kortshagen, Energy Environ. Sci. 2 (2009) 559–588.
- [11] X. Xia, J. Fu, Y. Zi, Nat. Commun. 10 (2019) 4428.
- [12] Z.L. Wang, J. Song, Science 312 (2006) 242–246.
- [13] W. Wu, L. Wang, Y. Li, F. Zhang, L. Lin, S. Niu, D. Chenet, X. Zhang, Y. Hao, T. F. Heinz, Nature 514 (2014) 470–474.
- [14] P. Reddy, S.-Y. Jang, R.A. Segalman, A. Majumdar, Science 315 (2007) 1568–1571.
- [15] M.H. Elsheikh, D.A. Shnawah, M.F.M. Sabri, S.B.M. Said, M.H. Hassan, M.B. A. Bashir, M. Mohamad, Renew. Sustain. Energy Rev. 30 (2014) 337–355.
- [16] F.-R. Fan, Z.-Q. Tian, Z.L. Wang, Nano Energy 1 (2012) 328–334.
- [17] G. Zhu, C. Pan, W. Guo, C.-Y. Chen, Y. Zhou, R. Yu, Z.L. Wang, Nano Lett. 12 (2012) 4960–4965.
- [18] J. Chen, Z.L. Wang, Joule 1 (2017) 480–521.
- [19] Q. Tang, M.-H. Yeh, G. Liu, S. Li, J. Chen, Y. Bai, L. Feng, M. Lai, K.-C. Ho, H. Guo, C. Hu, Nano Energy 47 (2018) 74–80.
- [20] Q. Tang, X. Pu, Q. Zeng, H. Yang, J. Li, Y. Wu, H. Guo, Z. Huang, C. Hu, Nano Energy 66 (2019) 104087.
- [21] Z. Lin, Z. Wu, B. Zhang, Y.-C. Wang, H. Guo, G. Liu, C. Chen, Y. Chen, J. Yang, Z. L. Wang, Adv. Mater. Technol. 4 (2018) 1800360.
- [22] Z. Lin, J. Yang, X. Li, Y. Wu, W. Wei, J. Liu, J. Chen, J. Yang, Adv. Funct. Mater. 28 (2018) 1704112.
- [23] W. Liu, Z. Wang, G. Wang, G. Liu, J. Chen, X. Pu, Y. Xi, X. Wang, H. Guo, C. Hu, Z. L. Wang, Nat. Commun. 10 (2019) 1426.
- [24] J. Wang, S. Li, F. Yi, Y. Zi, J. Lin, X. Wang, Y. Xu, Z.L. Wang, Nat. Commun. 7 (2016) 12744.
- [25] J. Yang, J. Chen, Y. Su, Q. Jing, Z. Li, F. Yi, X. Wen, Z. Wang, Z.L. Wang, Adv. Mater. 27 (2015) 1316–1326.
- [26] L. Lin, Y. Xie, S. Niu, S. Wang, P. Yang, Z.L. Wang, ACS Nano 9 (2015) 922–930.
- [27] G. Zhu, J. Chen, T. Zhang, Q. Jing, Z.L. Wang, Nat. Commun. 5 (2014) 3426.
- [28] C. Xu, Y. Zi, A.C. Wang, H. Zou, Y. Dai, X. He, P. Wang, Y. Wang, P. Feng, D. Li, Z. L. Wang, Adv. Mater. 30 (2018) 1706790.
- [29] Z. Lin, J. Chen, X. Li, Z. Zhou, K. Meng, W. Wei, J. Yang, Z.L. Wang, ACS Nano 11 (2017) 8830–8837.
- [30] Z. Lin, Y. Wu, Q. He, C. Sun, E. Fan, Z. Zhou, M. Liu, W. Wei, J. Yang, Nanoscale 11 (2019) 6802–6809.
- [31] L. Xu, T. Jiang, P. Lin, J. Shao, C. He, W. Zhong, X. Chen, Z.L. Wang, ACS Nano 12 (2018) 1849–1858.
- [32] Z. Lin, J. Chen, J. Yang, J. Nanomater. (2016) 1–24, 2016.
- [33] H. Ryu, J.H. Lee, U. Khan, S.S. Kwak, R. Hinchet, S.-W. Kim, Energy Environ. Sci. 11 (2018) 2057–2063.
- [34] H. Guo, J. Chen, M.-H. Yeh, X. Fan, Z. Wen, Z. Li, C. Hu, Z.L. Wang, ACS Nano 9 (2015) 5577–5584.
- [35] H. Zou, Y. Zhang, L. Guo, P. Wang, X. He, G. Dai, H. Zheng, C. Chen, A.C. Wang, C. Xu, Z.L. Wang, Nat. Commun. 10 (2019) 1427.